

Evolution of binaries producing Type Ia supernovae, luminous supersoft X-ray sources, and recurrent novae

Izumi Hachisu

College of Arts and Sciences, University of Tokyo, Meguro-ku, Tokyo
153-8902, Japan

Abstract. We have been proposing two evolutionary paths to Type Ia supernovae (SNe Ia), which are called the supersoft X-ray source (SSS) channel and the symbiotic channel, depending on the orbital separation just prior to an SN Ia explosion. The essential difference of our treatment is inclusion of strong, optically thick winds on mass-accreting white dwarfs (WDs) in the elementary processes of binary evolution when the mass accretion rate on to WDs exceeds a critical rate of $\dot{M}_{\text{cr}} \sim 1 \times 10^{-6} M_{\odot} \text{ yr}^{-1}$. Once optically thick winds begin to blow from the WD, the binary can avoid forming a common envelope in some cases. We call this *accretion wind*. So that the WDs are able to grow up to the Chandrasekhar mass and explode as an SN Ia, showing SSS or recurrent nova phenomena in the way to SNe Ia. Thus, the accretion wind process of WDs can open new channels to SNe Ia. We have modeled the LMC supersoft source RX J0513.9-6951 as an example of the systems in the accretion wind phase. Further inclusions of two other elementary processes make the channels much wider; these are the case BB mass transfer in the SSS channel and the strong orbital shrinkage during the superwind phase of the primary star in the symbiotic channel. As a result, the estimated birth rate of SNe Ia via these two channels becomes compatible with the observation in our Galaxy. Interestingly, the U Sco and T CrB subclasses of recurrent novae can be naturally understood as a part of evolutionary stages in these two SSS and symbiotic channels to SNe Ia, respectively. Thus we have a unified picture of binary evolutions to SNe Ia, luminous SSS, and recurrent novae.

1. Introduction

Type Ia supernovae (SNe Ia) are one of the most luminous explosive events of stars. Recently, SNe Ia have been used as good distance indicators that provide a promising tool for determining cosmological parameters (Perlmutter et al. 1999; Riess et al. 1998) because of their almost uniform maximum luminosities. However, one of the most important unresolved problems on SNe Ia is that we do not know the exact progenitor systems of SNe Ia.

It is widely accepted that the exploding star itself is an accreting white dwarf (WD) in a binary (Nomoto 1982; Nomoto, Thielemann, & Yokoi 1984). However, the companion star (and thus the observed binary system) is not known. Several

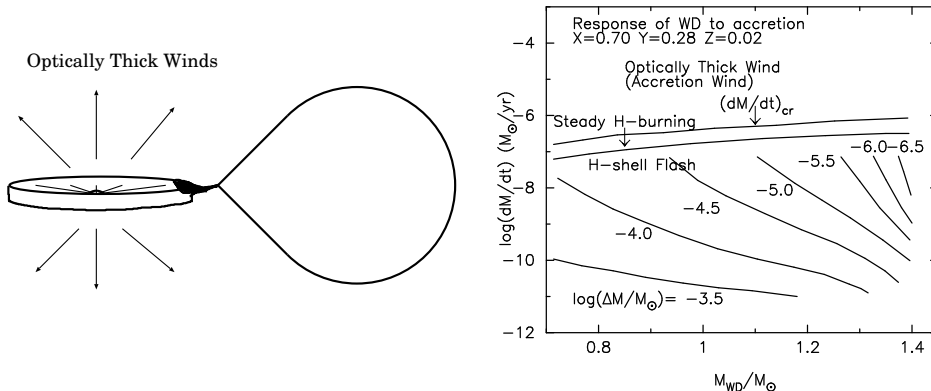


Figure 1. **Left:** Optically thick winds blow from mass-accreting white dwarfs when the mass transfer rate exceeds a critical rate, i.e., $M_{\text{acc}} > M_{\text{cr}}$. Here, we assume that the white dwarf accretes mass from equatorial region and, at the same time, blows winds from polar regions. **Right:** Response of white dwarfs to mass accretion is illustrated in the white dwarf mass and the mass accretion rate plane, i.e., in the $M_{\text{WD}}-M_{\text{acc}}$ plane. Strong optically thick winds blow above the line of $M_{\text{acc}} > M_{\text{cr}}$. There is no steady state burning below $M_{\text{acc}} < M_{\text{std}}$. Instead, intermittent shell flashes occur. The envelope mass at which hydrogen ignites to flash is also shown (taken from Fig. 9 of Nomoto 1982).

objects have ever been considered, which include merging double white dwarfs (Iben & Tutukov 1984; Webbink 1984), recurrent novae (Starrfield, Sparks, & Truran, 1985), symbiotic stars (Munari & Renzini 1992) etc (Livio 2000, for recent summary).

Among these models, the systems of double white dwarfs (the double degenerate model) are not theoretically supported; when two WDs merge, carbon ignites not at the center but near the surface layer of the C+O WD; so that the C+O WD is converted into an O+Ne+Mg WD (Saio & Nomoto 1998). If the total mass of the merger exceeds the Chandrasekhar mass, the merged WD does not explode as an SN Ia but collapses to a neutron star (Nomoto & Kondo 1991).

On the other hand, the single degenerate systems has become more promising, in which a C+O WD gains mass from a non-degenerate companion star and grows its mass up to the Chandrasekhar mass. Such promising progenitors include luminous supersoft X-ray sources (SSS), recurrent novae (RNe), and symbiotic stars. However, the most important problem in these single degenerate systems is that we did not know the mechanism how to grow the mass of the WDs. Instead, there are effective mass-losing mechanisms such as nova ejection and common envelope evolutions that get rid of the mass accumulated on the WD. Here, I review and summarize our recent developments of the mechanisms that enable to grow the mass of WDs in the single degenerate systems and give a unified picture of evolutions of SSSs, recurrent novae, and SNe Ia.

2. Accretion wind evolution

First, we briefly explain how the mass of WDs in the single degenerate systems grow toward the Chandrasekhar mass limit. The reason that the standard binary evolution theory fails to explain the evolutionary path to SNe Ia and recurrent novae lies mainly in the theoretical prediction of a common envelope formation and the ensuing spiral-in process, because these processes inhibit the growth of white dwarfs in binary systems. As discussed in many previous papers on binary evolution, it has been widely accepted that a hydrogen-rich envelope on a mass-accreting white dwarf expands to a red giant size when its mass accretion rate, \dot{M}_{acc} , exceeds a critical limit, i.e.,

$$\dot{M}_{\text{cr}} = 8.3 \times 10^{-7} \left(\frac{M_{\text{WD}}}{M_{\odot}} - 0.4 \right) M_{\odot} \text{ yr}^{-1}, \quad (1)$$

(see, e.g., Fig. 9 of Nomoto 1982) and easily forms a common envelope. Once a common envelope is formed, two stars begin to spiral-in each other as a result of viscous drag, thus producing a double degenerate system (Iben & Tutukov 1984; Webbink 1984).

However, Hachisu, Kato, & Nomoto (1996) found that white dwarfs begin to blow strong winds ($v_{\text{wind}} \sim 1000 \text{ km s}^{-1}$ and $\dot{M}_{\text{wind}} > 1 \times 10^{-6} M_{\odot} \text{ yr}^{-1}$) when $\dot{M}_{\text{acc}} > \dot{M}_{\text{cr}}$, as illustrated in Fig. 1, thus preventing the binary from collapsing. The binary does not spiral-in but keeps its separation. Hydrogen burns steadily, and therefore the helium layer of the white dwarf can grow at a rate of $\dot{M}_{\text{He}} \approx \dot{M}_{\text{cr}}$. The other transferred matter is blown in the wind ($\dot{M}_{\text{wind}} \approx \dot{M}_{\text{acc}} - \dot{M}_{\text{cr}}$), where \dot{M}_{wind} is the wind mass loss rate. We call this *accretion wind* because it begins to blow when the accretion rate exceeds the critical rate.

Therefore, we have to revise Fig. 9 of Nomoto (1982), which has been used widely in binary evolution scenarios to show the basic processes of mass-accreting white dwarfs. The revision to Nomoto's Fig. 9 is shown in Fig. 1. The most important difference of Fig. 1 from Nomoto's Fig. 9 is that white dwarfs increase their masses in a much wider parameter region. In our new diagram, the status of a mass-accreting white dwarf is specified by the following three phases: (1) accretion wind phase ($\dot{M}_{\text{acc}} > \dot{M}_{\text{cr}}$); (2) steady shell-burning phase ($\dot{M}_{\text{std}} < \dot{M}_{\text{acc}} < \dot{M}_{\text{cr}}$); and (3) intermittent shell-flash phase ($\dot{M}_{\text{acc}} < \dot{M}_{\text{std}}$), where \dot{M}_{std} means the lowest limit of the mass accretion rate for steady hydrogen shell-burning. The new growing region of white dwarfs, $\dot{M}_{\text{acc}} > \dot{M}_{\text{std}}$, is much wider than old Nomoto's (1982) narrow strip, $\dot{M}_{\text{std}} < \dot{M}_{\text{acc}} < \dot{M}_{\text{cr}}$.

2.1. RX J0513.9-6951 as an example of accretion wind phase

As an example of the *accretion wind* phase, we have modeled long-term optical light curves of the LMC supersoft X-ray source RX J0513.9-6951 based on our wind model of mass-accreting white dwarfs. The source shows a quasi-periodic variability, the period of which is $\sim 170 \text{ d}$ and the amplitude of which is $\sim 1 \text{ mag}$ (Alcock et al. 1996). The source has a relatively longer ($\sim 130 \text{ d}$) optical high-state ($V \sim 16.2$) and a shorter ($\sim 40 \text{ d}$) optical low-state ($V \sim 17.0$) with the transition time of several days. X-rays were observed only in the optical low-states. This indicates that a strong wind blows only in the optical high-state

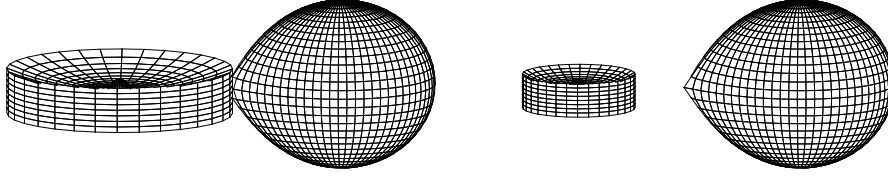


Figure 2. **Left:** Geometrical configuration of our RX J0513.9-6951 model in the optical high state (wind phase). The cool component is a slightly evolved MS companion filling up its inner critical Roche lobe. The hot component, WD, blows a strong wind. The accretion disk is blown off outward and has a larger size than the no-wind phase. **Right:** Geometrical configuration in the optical low state (no-wind phase).

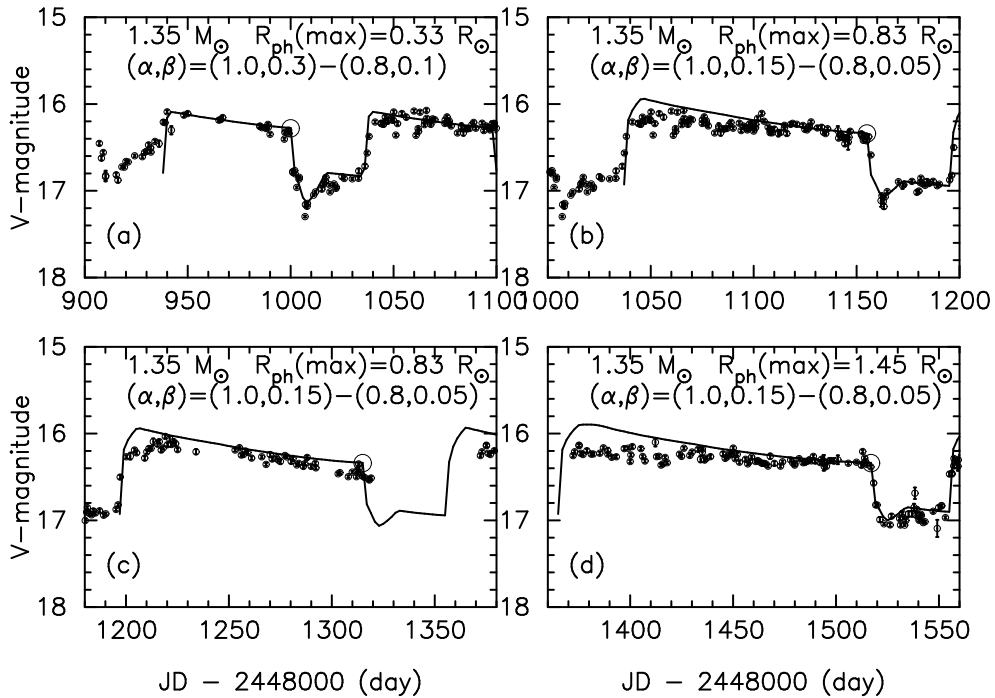


Figure 3. Light curve is plotted against time for a $1.35M_{\odot}$ white dwarf model together with the MACHO data (Alcock et al. 1996). We assume a larger size of the accretion disk (1.0 times the Roche lobe size) in the optical high state (the wind phase) but a smaller size (0.8 times the Roche lobe size) in the optical low state (the static, no-wind phase). The transition from the optical high to low state corresponds to the cease point of the strong wind (large open circles).

because X-rays are self-absorbed by the wind. To examine the idea of the strong wind, we have calculated envelope solutions of mass-accreting WDs and found that optically thick winds really occur when the mass accretion rate exceeds a critical rate of \dot{M}_{cr} for $M_{\text{WD}} > 0.7M_{\odot}$ even in a low metallicity of $Z = 0.004$ of LMC.

We attribute the 100 – 150 d bright phase to our strong wind phase with an expanded white dwarf photosphere, whereas the ~ 40 d less bright phase to our static (no-wind) phase with a shrinking envelope of the WD. The duration and the brightness of the optical high state is explained by the model of a WD mass, $M_{\text{WD}} = 1.35 M_{\odot}$, with an extending accretion disk edge over the Roche lobe size during the wind phase as illustrated in Fig. 2. Irradiation of the accretion disk by the WD photosphere plays an essential role to reproduce the optical light curve because a large part of the optical light comes from the accretion disk.

The switching mechanism from the optical high to low state is understood as follows: Strong winds from the WD themselves make the separation increase, because the high velocity wind do not carry away large angular momentum. The winds further strip off the very surface layer of the companion star. As a result, the mass transfer rate decreases and it finally stops the strong winds. After the wind stops, the surface of the companion recovers in a thermal timescale of the envelope and the mass transfer rate increases up and strong winds begin to blow again. Thus, the semi-periodic cycles repeat.

Light curve fittings indicate that the optical high state is initiated by a sudden increase in the mass transfer rate of $\dot{M}_{\text{acc}} \sim 1 \times 10^{-5} M_{\odot}$. Then, the envelope of the white dwarf expands to $R_{\text{ph}} \sim 0.1 R_{\odot}$, not exceeding over the accretion disk size of $\sim 2 R_{\odot}$. Our light curve fittings are shown in Fig. 3. In our models, about 40% of the transferred matter can be accumulated on the white dwarf but the rest is blown off in the wind. This suggests that it takes $\sim 1 \times 10^5$ yr for the white dwarf of $1.35 M_{\odot}$ to grow to $1.38 M_{\odot}$ and to explode as a Type Ia supernova.

2.2. Two evolutionary paths to RNe and SNe Ia

Based on the new mechanism of the accretion wind evolution as shown in Fig. 1, Hachisu, Kato, & Nomoto (1999a) and Hachisu et al. (1999b) have proposed two paths to SNe Ia (see also, Li & van den Heuvel 1997). In these two paths, WDs can accrete mass continuously from the companion and grow at a rate of \dot{M}_{cr} of eq. (1). Therefore, candidates for SN Ia progenitors are systems at the final stages on these paths; i.e., one is a supersoft X-ray source (SSS) consisting of a WD and a lobe-filling, more massive, main-sequence (MS) companion as shown in the late stage of Fig. 4 (the WD+MS systems; see also Li & van den Heuvel 1997) and the other is a symbiotic star consisting of a WD and a mass-losing red giant (RG) as shown in the late stage of Fig. 5 (the WD+RG systems, see also Hachisu et al. 1996). Both the systems contribute to main parts of the SN Ia birth rate (Hachisu et al. 1999a, 1999b).

Hachisu et al. (1999a, 1999b) have followed many binary evolutions until SN Ia explosions. The final outcome is summarized in Fig. 6 for the initial orbital period, P_0 (in units of days), and the initial donor mass, $M_{d,0}$, which is representing $M_{\text{RG},0}$ (the initial mass of the red-giant component), or $M_{\text{MS},0}$ (the

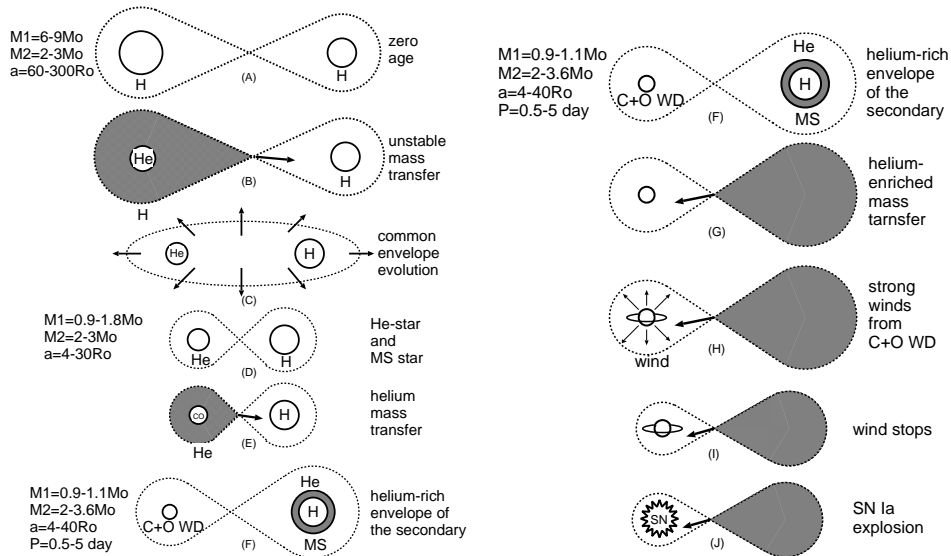


Figure 4. SSS channel. **Left:** Early evolutionary path through the common envelope evolution to the helium (Case BB) mass transfer. **Right:** Late evolutionary path to an SN Ia explosion in our wind model.

initial mass of the slightly evolved main-sequence component). In this figure, the initial mass of the white dwarf is assumed to be $M_{\text{WD},0} = 1.0M_{\odot}$. The right-hand region, longer orbital periods of $P_0 \sim 100-1000$ d, represents our results for the WD+RG system. In the left-hand region, shorter orbital periods of $P_0 \sim 0.3-10$ d, are shown the results for the WD+MS system.

We plot the initial parameter regions of binaries (thin solid curves in Fig. 6) that finally produce an SN Ia, which are corresponding to stage (F) in Fig. 4 or stage (D) in Fig. 5. Left diagram in Fig. 6 shows such two regions of the WD+MS systems (SSS channel) and the WD+RG systems (symbiotic channel). We have added in this figure the final parameter regions (thick solid curves) just before an SN Ia explosion occurs. Starting from the initial region encircled by the thin solid curves, binary systems evolve and can explode as an SN Ia in the regions enclosed by the thick solid curves. Hachisu & Kato (2001) showed that some recurrent novae lie on the boarder of their parameter region that can produce an SN Ia (see also Kato 2001 in this volume). Among six recurrent novae with known orbital periods, five fall in the final regions of SN Ia progenitors just before the explosion. Only T Pyx is far out of the regions of SNe Ia.

3. Case BB mass transfer

It has been shown that the ejecta of the recurrent nova U Sco are helium-rich as much as $\text{He}/\text{H} \sim 2$ by number (Williams et al. 1981). The accretion disk of U Sco is also suggested to be helium-rich (Hanes 1985). Many of the SSSs have a stronger He II line than Balmer lines, thus also suggesting that the companion of the WD+MS systems (SSS channel) is helium-rich. In this section, therefore,

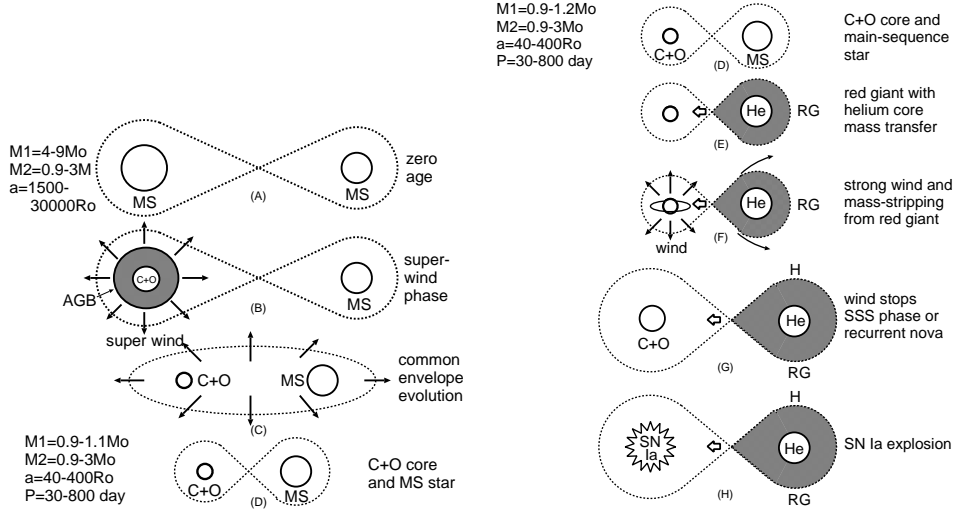


Figure 5. Symbiotic channel. **Left:** Early evolutionary path through the first common envelope evolution to a symbiotic system. **Right:** Late evolutionary path through the symbiotic channel to an SN Ia.

we describe the reason that the cool component of the WD+MS systems has a helium-rich envelope.

Previous works consider only the initial systems consisting of a more massive AGB star with a C+O core and a less massive main-sequence star. This system undergoes a common envelope evolution and it finally yields a binary system of a mass-accreting C+O WD and a lobe-filling MS/subgiant star. Thus, they do not include another important evolutionary path, in which a more massive component fills up its inner critical Roche lobe when it develops a *helium core* of $\sim 0.8 - 2.0M_\odot$ in its *red giant phase* as shown in the early stage of Fig. 4.

We consider, for example, a close binary with the primary mass of $M_{1,i} = 7M_\odot$ and the secondary mass of $M_{2,i} = 2M_\odot$ with the initial separation of $a_i \sim 80 - 600 R_\odot$. When the primary has evolved to a red giant developing a helium core of $M_{1,\text{He}} \sim 1.0 - 1.6M_\odot$, it fills up its inner critical Roche lobe. Then, the binary undergoes a common envelope (CE) evolution, which yields a much more compact close binary of a naked helium star of $M_{1,\text{He}} \sim 1.0 - 1.6M_\odot$ and a main-sequence star of $M_2 = 2M_\odot$ with the final separation of $a_{f,\text{CE}} \sim 4 - 50 R_\odot$. Here, we assume a relation of

$$\frac{a_{f,\text{CE}}}{a_i} \sim \alpha_{\text{CE}} \left(\frac{M_{1,\text{core}}}{M_{1,i}} \right) \left(\frac{M_2}{M_{1,i} - M_{1,\text{core}}} \right), \quad (2)$$

with the efficiency factor of $\alpha_{\text{CE}} = 1.0$ for the common envelope evolutions.

After the common envelope evolution, the radii of the inner critical Roche lobes of the primary and the secondary become $R_1^* \sim 0.36a_{f,\text{CE}}$ and $R_2^* \sim 0.4a_{f,\text{CE}}$, respectively. Since the secondary radius should be smaller than its inner critical Roche lobe, i.e., $1.7R_\odot \leq R_2 < R_2^*$ ($1.7R_\odot$ is the radius of a $2M_\odot$ ZAMS star), the initial separation a_i should exceed $80 R_\odot$. The upper bound

of the initial separation is obtained from the maximum radius of the $7M_{\odot}$ star which has formed a helium core, i.e., $a_i \approx 2R_{1,\max} < 2 \times 300 R_{\odot}$. Thus, the allowable range of the initial separations is $80 R_{\odot} < a_i < 600 R_{\odot}$ for a pair of $M_{1,i} = 7M_{\odot}$ and $M_{2,i} = 2M_{\odot}$. Then, we have $R_1^* \sim 1.5 - 18 R_{\odot}$ and $R_2^* \sim 1.7 - 20 R_{\odot}$ after the first common envelope evolution.

After the hydrogen-rich envelope is stripped away and hydrogen shell burning vanishes, the naked helium core contracts to ignite a central helium burning and becomes a helium main sequence star. When the helium star forms a C+O core, its helium envelope expands to fill its inner critical Roche lobe again. The helium is transferred stably to the secondary on an *evolutionary time scale* of $\tau_{\text{EV}} \sim 10^5$ yr because the mass ratio is smaller than 0.79 ($q = M_1/M_2 < 0.79$). The resultant mass transfer rate is $\dot{M}_1 \sim 10^{-5} M_{\odot} \text{ yr}^{-1}$. No common envelope is formed for such a low rate. After the helium envelope is lost, the primary becomes a C+O WD of $M_{\text{C+O}} \sim 0.9 - 1.1M_{\odot}$ and the separation increases by 10%–40%, i.e., $a_{f,\text{He}} \sim (1.1 - 1.4)a_{f,\text{CE}} \sim (4 - 70)R_{\odot}$. Here, we assume the conservations of the total mass and angular momentum during the helium mass transfer to obtain the separation after the helium mass transfer, $a_{f,\text{He}}$. The secondary receives almost pure helium matter of $\Delta M_{\text{He}} \sim 0.1 - 0.5M_{\odot}$ to form a helium-enriched envelope. The secondary’s hydrogen content decreases to $X \sim 0.6$ if helium is completely mixed into the star. For the $9 + 2.5M_{\odot}$ case, much more helium is transferred, but much less helium for the $6 + 2M_{\odot}$ case.

4. Shrink of orbital separation during superwind phase

Based on the population synthesis analysis, Yungelson & Livio (1998) claimed that almost no realization frequency is derived for the original WD+RG model (Hachisu et al. 1996). In this section, we point out that very wide binaries with initial separations of $a_i > 1500 R_{\odot}$, which were not included in their analysis, are essentially important in our SN Ia modeling.

The more massive component (the initial mass of $M_{1,i}$) of a binary first evolves to a red giant (AGB stage) and fills its inner critical Roche lobe. After a common envelope phase, the more massive component leaves a C+O WD, and the separation of the binary decreases by a factor of $a_f/a_i \sim 1/40 - 1/50$ from eq.(2) for $M_{\text{WD}} \sim 1 M_{\odot}$ and $M_2 \sim 1 M_{\odot}$ because a $\sim 1 M_{\odot}$ WD descends from a main-sequence star of $M_{1,i} \sim 7 - 8 M_{\odot}$. Yungelson & Livio (1998) assumed that the separation of interacting binaries is *smaller than* $a_i < 1500 R_{\odot}$. Then, the widest binaries have separations of $a_f < 30 - 40 R_{\odot}$ after common envelope evolution. The orbital period is $P_0 < 20$ days for $M_{\text{WD},0} \sim 1 M_{\odot}$ and $M_{\text{RG},0} \sim 1 M_{\odot}$. There is no SN Ia region of the WD+RG systems for $P_0 < 20$ days as seen from Fig. 6. Thus, Yungelson & Livio concluded that we cannot expect any SN Ia explosions from the right-hand SN Ia region (WD+RG system) in Fig. 6.

The reason that Yungelson & Livio’s modeling fails to reproduce our SN Ia progenitors is their assumption of $a_i < 1500 R_{\odot}$. In what follows, we show that WD+RG binaries wide enough to have $P_0 \sim 100 - 1000$ d are born from initially very wide binaries with $a_i \sim 1500 - 40000 R_{\odot}$.

A star with a zero-age main-sequence mass of $M_{1,i} < 8 M_{\odot}$ ends its life by ejecting its envelope in a wind of relatively slow velocities ($v \sim 10 - 40 \text{ km s}^{-1}$)

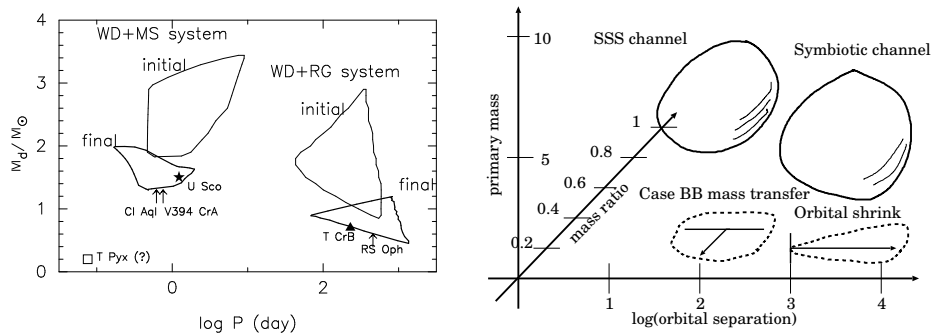


Figure 6. **Left:** Regions producing SNe Ia are plotted in the $\log P - M_d$ (orbital period — donor mass) plane for the WD+MS system (*left*) and the WD+RG system (*right*). Here we assume an initial white dwarf mass of $1.0M_\odot$. Currently known positions of each recurrent nova are indicated by a star mark (\star) for U Sco (Hachisu et al. 2000), a filled triangle for T CrB (Belczyński & Mikolajewska 1998), an open rectangle for T Pyx (Patterson et al. 1998), but by arrows for the other three recurrent novae, V394 CrA, CI Aql, and RS Oph, because the mass of the companion is not yet available explicitly. **Right:** The accretion winds of WDs open new two channels to SNe Ia while the two evolutionary processes of the case BB mass transfer and the orbital shrinkage during the superwind phase enlarge the initial phase volume of SN Ia progenitors for the SSS channel and the symbiotic channel, respectively.

as shown in Fig. 5. These wind velocities are as low as the orbital velocities of binaries with separations of $a_i \sim 1500 - 40000 R_\odot$ for a pair of $M_{1,i} \sim 7 M_\odot$ and $M_{2,i} \sim 1 M_\odot$. When the wind velocity is as low as the orbital velocity, we have the separation shrinking due to effective loss of the angular momentum by the outflowing gas, i.e., $\dot{a}/a \approx 2\dot{M}_1/M_2 < 0$ (see Hachisu et al. 1999a).

Once the binary system begins to shrink, its evolution becomes similar to a common envelope evolution (see *stages B-D* in Fig. 5). Thus, the separation is reduced by a factor of $1/40 - 1/50$, i.e., $a_f \sim 30 - 1000 R_\odot$ for $M_{1,i} \sim 7 M_\odot$ and $M_{2,i} \sim 1 M_\odot$. The orbital period becomes $P_0 \sim 15 - 3000$ days for a pair of $M_{WD,0} \sim 1 M_\odot$ and $M_2 \sim 1 M_\odot$ (*stage D* in Fig. 5). These initial sets of the parameters are very consistent with the initial conditions of our WD+RG progenitor systems.

5. Type Ia supernova rates

We estimate the SN Ia rate from the WD+RG and WD+MS systems in our Galaxy by

$$\nu = 0.2 \int dq \int d \log A \int \frac{dM}{M^{2.5}} \text{ yr}^{-1}, \quad (3)$$

where q , A , and M are the mass ratio ($q = M_2/M_1 \leq 1$), the initial separation in units of solar radius, and the primary initial mass in solar mass units (from

eq. [1] of Iben & Tutukov 1984). The SN Ia rate is essentially the same as the volume of the initial phase space consisting of q , A , and M as shown in Fig. 6.

The accretion winds of WDs open new two channels to SNe Ia. The case BB mass transfer in the SSS channel extends the phase volume towards the low mass ratio region as shown in Fig. 6. On the other hand, the orbital shrinkage during the superwind phase in the symbiotic channel enlarges the phase space towards the large initial separation also shown in Fig. 6. Therefore, the estimated rate of WD+RG/WD+MS systems becomes close to the observed rate in our Galaxy, i.e., $\nu \sim 0.003 \text{ yr}^{-1}$, which comes from the SSS channel of $\nu_{\text{MS}} \sim 0.001 \text{ yr}^{-1}$ and the symbiotic channel of $\nu_{\text{RG}} \sim 0.002 \text{ yr}^{-1}$.

References

- Alcock, C. et al. 1996, MNRAS, 280, L49
 Belczyński, K., & Mikolajewska, J. 1998, MNRAS, 296, 77
 Hachisu, I., & Kato, M. 2001, ApJ, 558, 323
 Hachisu, I., Kato, M., Kato, T., & Matsumoto, K. 2000, ApJ, 528, L97
 Hachisu, I., Kato, M., & Nomoto, K. 1996, ApJ, 470, L97
 Hachisu, I., Kato, M., & Nomoto, K. 1999a, ApJ, 522, 487
 Hachisu, I., Kato, M., Nomoto, K., & Umeda, H. 1999b, ApJ, 519, 314
 Hanes, D. A. 1985, MNRAS, 213, 443
 Iben, I. Jr., & Tutukov, A. V. 1984, ApJS, 54, 335
 Kato, M. 2001, in The Physics of Cataclysmic Variables and Related Objects (this volume), in press
 Livio, M. 2000, in Type Ia Supernovae: Theory and Cosmology, ed. J. C. Niemeyer & J. W. Truran (Cambridge: Cambridge Univ. Press), 33
 Li, X.-D., & van den Heuvel, E. P. J. 1997, A&A, 322, L9
 Munari, U., & Renzini, A. 1992, ApJ, 397, L87
 Nomoto, K. 1982, ApJ, 253, 798
 Nomoto, K., & Kondo, Y. 1991, ApJ, 367, L19
 Nomoto, K., Thielemann, F., & Yokoi, K. 1984, ApJ, 286, 644
 Patterson, J. et al. 1998, PASP, 110, 380
 Perlmutter, S. et al. 1999, ApJ, 1999, 517, 565
 Riess, A. G. et al. 1998, AJ, 116, 1009
 Saio, H., & Nomoto, K. 1998, ApJ, 500, 388
 Starrfield, S., Sparks, W. M., & Truran, J. W. 1985, ApJ, 291, 136
 Webbink, R. F. 1984, ApJ, 277, 355
 Williams, R. E., Sparks, W. M., Gallagher, J. S., Ney, E. P., Starrfield, S. G., & Truran, J. W. 1981, ApJ, 251, 221
 Yungelson, L., & Livio, M. 1998, ApJ, 497, 168